Research Article Vol. 31, No. 5 / 27 Feb 2023 / Optics Express 8226
Optics EXPRESS

Design of an interferometric fiber optic parametric amplifier for the rejection of unwanted four-wave mixing products

VLADIMIR GORDIENKO,[1,*] FILIPE M. FERREIRA,[2] VITOR RIBEIRO,[1,3] AND NICK DORAN[1]

[1]Aston Institute of Photonic Technologies, Aston University, Birmingham, B4 7ET, UK
[2]Optical Networks Group, University College London, London, WC1E 6BT, UK
[3]Now with Kets Quantum Security LTD, Bristol, BS15 4PJ, UK
[*]v.gordienko1@aston.ac.uk

Abstract: We introduce a novel (to our knolwedge) interferometric fiber optic parametric amplifier (FOPA), allowing for the suppression of unwanted four-wave mixing products. We perform simulations of two configurations where one rejects idlers and, the other rejects nonlinear crosstalk from the signal output port. The numerical simulations presented here demonstrate the practical feasibility of suppressing idlers by >28 dB across at least 10 THz enabling the reuse of the idler frequencies for signal amplification and thus doubling the employable FOPA gain bandwidth. We demonstrate it can be achieved even when the interferometer employs real-world couplers by introducing a small attenuation in one of the interferometer arms.

1. Introduction

The rapid development of multiband optical communications [1] fuels research of novel optical amplifiers having large bandwidth (e.g. > 10 THz) and operating in frequency bands lacking suitable amplifiers (e.g. O/E/S). The fiber optic parametric amplifier (FOPA) is the perfect candidate to satisfy this demand due to its abilities to operate in an (almost) arbitrary wavelength range and with theoretically unconstrained gain bandwidth [2]. Thus, experimental FOPA demonstrations include operation in all of O, E, S, C and L bands [3] and with gain bandwidth of more than 100 nm (>12 THz) [4,5,6]. Moreover, the FOPA can support future expansions of transmission bandwidth in other bands, for example, facilitated by hollow core fibers with ultra-wide low attenuation window [7].

One of key FOPA challenges is the generation of many unwanted four wave mixing products during amplification: the idlers and the nonlinear crosstalk. The idlers are spectrally inverted signal copies produced during signal amplification, and the nonlinear crosstalk products emerge from four wave mixing between two and more signals or idlers. An overlap between the signals and idlers is commonly avoided in WDM systems by keeping signals to one side of the FOPA central frequency [8], although signal and idler bands can be distributed across the FOPA gain bandwidth in different ways [9]. Either way, idlers block up to a half of the FOPA gain bandwidth, thus halving gain bandwidth employable for signal amplification. The nonlinear crosstalk power is lower than that of idlers, and they can be reduced in several ways [10,11,12], but nonlinear crosstalk remains a major source of signal degradation and the key factor limiting the output signal power [13].

In this paper, we introduce two FOPA architectures based on Mach-Zehnder interferometer which guide signals and unwanted four wave mixing products (idlers and the first-order nonlinear crosstalk respectively) into different output ports. Interferometric rejection of idlers removes

#476884 https://doi.org/10.1364/OE.476884
Journal © 2023 Received 5 Oct 2022; revised 8 Feb 2023; accepted 8 Feb 2023; published 21 Feb 2023

Optics EXPRESS

the requirement to reserve a band for idlers and allows signals to occupy the whole FOPA gain bandwidth thus doubling the employable FOPA gain bandwidth. Interferometric rejection of the first-order nonlinear crosstalk products significantly mitigates this source of signal degradation and facilitates linear FOPA operation at much higher output signal power. Although a range of interferometric architectures for parametric devices has been studied previously in [14,15,16,17,18,19], here we suggest the novel concept of employing a nonlinear interferometer for broadband rejection of idlers and nonlinear crosstalk from FOPAs amplifying WDM signals. We perform simulations to confirm the concept and to evaluate its feasibility aiming for idlers suppression by >28 dB, which is sufficient to amplify 16QAM signals at idlers' wavelengths with required OSNR penalty <0.3 dB at BER of 10^{-3}. Since this level of suppression requires tight margins on the coupling coefficients in a plain interferometer, we demonstrate two simple techniques enabling idlers suppression by >28 dB across bandwidth over 10 THz with relaxed requirements for couplers, e.g. the coupler coefficient varies in the range between 0.48 and 0.5 across the FOPA gain bandwidth in our example.

2. Concept

Figure 1 shows a comparison of an ordinary and interferometric FOPAs for rejection of nonlinear crosstalk and idlers. Rejection of nonlinear crosstalk allows to mitigate this impairment in FOPA. Rejection of idlers allows to double the FOPA gain bandwidth employable for signal amplification. Note, the concept is explained in the context of phase-insensitive FOPAs, although it is applicable to phase-sensitive FOPAs too.

2.1. Ordinary FOPA

In an ordinary FOPA the pump and the signals are coupled with a wavelength-selective multiplexer (λ-MUX), then the signals are amplified in a highly nonlinear fiber (HNLF) as shown at Fig. 1(a). Nonlinear crosstalk and idlers are unwanted FWM products of the signal amplification process. Nonlinear crosstalk products occurring at signal frequencies degrade signal-to-noise ratio and they cannot be demultiplexed from signals in an ordinary FOPA. Although idlers are commonly demultiplexed from signals by a wavelength-selective demultiplexer (λ-DEMUX), e.g. a filter, the idlers block up to a half of a FOPA gain bandwidth and make it unavailable for signal amplification.

2.2. Symmetric MZI-FOPA for rejection of nonlinear crosstalk

A FOPA employing a symmetric MZI shown at Fig. 1(b) mitigates nonlinear crosstalk by guiding the first-order nonlinear crosstalk products and the signals to different output ports of the MZI. The first-order nonlinear crosstalk products are the most significant because they involve the pump wave. Besides, the MZI-FOPA improves noise figure by combining the pump and the signals via a virtually lossless 3 dB coupler instead of a lossy wavelength-selective multiplexer. Indeed, although a 3 dB coupler does introduce a 3 dB signal attenuation in each arm, this is compensated by the coherent addition of signal at the interferometer output, i.e. a MZI does not degrade noise figure except for excess loss.

Schematic diagrams show evolution of optical spectra and phases along the MZI-FOPA (Fig. 1(b)). A pump and input signals are injected in different input ports of a MZI and mixed by a 3 dB coupler (diagrams b1 and b2). The coupler introduces π/2 phase shifts to the signals and the pump as shown by the diagrams b3 and b4. Each arm of the MZI employs identical sections of highly nonlinear fiber (HNLF) where signals are amplified and collateral idlers and nonlinear crosstalk products are generated. The pump and the signal phases at the input of HNLF sections define the relative idler and nonlinear crosstalk phases after the HNLF. The relative idler phases are shown at the diagrams b5 and b6 according to Eq. (1), where φ_p, φ_s and φ_i are the pump, signal and idler phases respectively. This relation is due to the idler optical field E_i

Optics EXPRESS

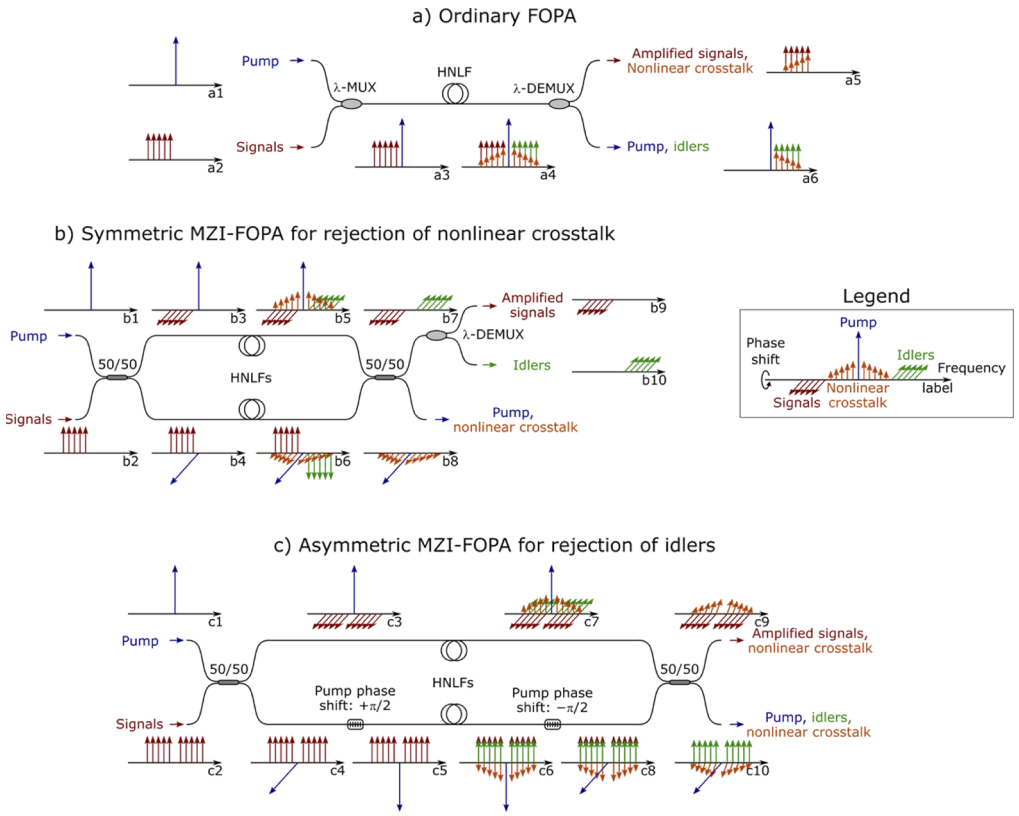

Fig. 1. Comparison of a) an ordinary FOPA with b) FOPA in symmetric Mach-Zehnder interferometer (MZI) for rejection of nonlinear crosstalk and c) FOPA in asymmetric MZI for rejection of idlers. Evolution of optical spectra along FOPAs is shown by labelled schematic diagrams. Frequencies and relative phase shifts of the signals (red), the pump (blue), the idlers (green) and the first-order nonlinear crosstalk (orange) are illustrated by position and rotation of corresponding arrows respectively. Rejection of nonlinear crosstalk improves signal-to-noise ratio, and rejection of idlers allows to double the FOPA gain bandwidth employable for signal amplification. Besides, interferometric FOPAs have lower noise figure and insertion loss than ordinary FOPAs due to replacement of lossy multiplexers with virtually lossless 3 dB couplers.

Optics EXPRESS

being proportional to $E_p{}^2 \cdot E_s{}^*$, where E_p and E_s are the optical fields of the pump and the signal respectively [20].

The first-order nonlinear crosstalk products occur due to the following four wave mixing processes $E_s \cdot E_p \cdot E_s{}^*$, $E_i \cdot E_p \cdot E_i{}^*$ and $E_s \cdot E_i \cdot E_p{}^*$ [20]. Phases of these crosstalk products scale with the pump phase only as shown by Eqs. (2–4) and reflected at the diagrams b5 and b6. Then, all waves from each arm add with their corresponding waves from another arm in the output 3 dB coupler. Considering diagonal π/2 phase shifts, the signals and the idlers fully recombine at one output port (b7), while the pump and the first-order nonlinear crosstalk fully cancel out at the signal output port (b7). Indeed, the first-order nonlinear crosstalk products from different MZI arms appear to be in counter-phase at b7, and hence get mitigated. However, a wavelength-selective filter is required to demultiplex signals and idlers at the MZI-FOPA output.

$$\varphi_i \sim 2 \cdot \varphi_p - \varphi_s, \tag{1}$$

$$\varphi_{XT,1} \sim \varphi_s + \varphi_p - \varphi_s = \varphi_p, \tag{2}$$

$$\varphi_{XT,2} \sim \varphi_i + \varphi_p - \varphi_i = \varphi_p, \tag{3}$$

$$\varphi_{XT,3} \sim \varphi_s + \varphi_i - \varphi_p \sim \varphi_s + (2 \cdot \varphi_p - \varphi_s) - \varphi_p = \varphi_p. \tag{4}$$

2.3. Asymmetric MZI-FOPA for rejection of idlers

A FOPA employing an asymmetric MZI (Fig. 1(c)) can guide signals and idlers to different MZI output ports, so there is no need to reserve a half of the FOPA gain bandwidth for idlers. Indeed, ordinary FOPAs typically amplify a band of signals on one side of the pump and reserve a band symmetric around the pump for idlers. However, an asymmetric MZI-FOPA rejecting idlers can employ the whole FOPA gain bandwidth on both sides of the pump for signal amplification, because idlers occurring within these bands cancel at the signal output due to interference (the idlers constructively recombine at the other MZI output). Consequently, the asymmetric MZI-FOPA can employ twice the bandwidth for signal amplification as compared to an ordinary FOPA as shown by diagrams a2 and c2 at Fig. 1. The asymmetric MZI-FOPA provides a noise figure improvement similarly to the symmetric MZI-FOPA due to lack of a lossy multiplexer at the input. Besides, the asymmetric MZI-FOPA has the lowest insertion loss of the three compared FOPA configurations due to lack of a lossy multiplexer at the output as well. Finally, the asymmetric MZI-FOPA provides a 3 dB reduction of the first-order nonlinear crosstalk by splitting them equally between the output ports.

The asymmetric MZI-FOPA is similar to the symmetric MZI-FOPA but includes two pump phase shifters in one of its arms and can amplify signals across the whole FOPA gain spectrum as shown by the diagram c2 at Fig. 1(c). The input coupler combines the pump with the signals and adds π/2 phase shifts as shown by the diagrams c3 and c4. Then, the pump phase in one of arms is shifted by π/2 to introduce an asymmetry (diagram c5). This can be done by a fiber Bragg grating (FBG) with reflection band close to the pump frequency similarly to quasi-phase matched FOPAs [21]. Then, the idlers and nonlinear crosstalk products generated during signal amplification inherit the additional pump phase shift according to Eqs. (1–4) as shown by the diagrams c6 and c7. Then, the same pump phase is shifted by -π/2 to compensate for the previous shift and to ensure the pump cancellation at the signal output port (c8). At that stage signals and idlers occur at the same frequencies and get mixed in both arms (diagrams c7 and c8), but idlers in the upper arm are π/2 *behind* idlers in the bottom arm, while signals in the upper arm are π/2 *ahead* of signals in the bottom arm. This is the crucial relation leading to signals and idlers recombination at different output ports of the MZI-FOPA. Hence, the cancellation of idlers at the signal output port makes the whole FOPA gain bandwidth available for signal amplification. Note, that nonlinear crosstalk products do not cancel out at either output port but split equally between them. However, this implies a 3 dB reduction of nonlinear crosstalk power at the signal output port as compared to an ordinary FOPA.

Optics EXPRESS

2.4. Feasibility considerations of MZI-FOPA

A Mach-Zehnder interferometer (MZI) is preferred for interferometric FOPAs instead of Sagnac interferometer because the latter incurs significant implementation penalties in FOPAs. Thus, FOPAs in Sagnac loops with a single gain stage are not feasible due to detrimental coupling between FWM and stimulated Brillouin scattering [22]. An employment of two or more gain stages in looped FOPAs allows to avoid this coupling but variants of this configuration significantly increase nonlinear crosstalk and/or noise figure [13]. It should be noted that a typical gain fiber length in FOPA is of the order of 100 m, so stabilization of such a long Mach-Zehnder interferometer can be a concern. However, a recent experimental demonstration of polarization-insensitive FOPA in a Mach-Zehnder arrangement confirms a practical feasibility of the required stabilization [23].

The same setup can be used for two-pump FOPAs. However, for idler rejection either a phase-shifter for each pump is required, or a double phase shift, i.e. π, has to be applied to a single pump.

3. Simulations of ideal MZI-FOPAs

In this section we perform simulations to confirm rejection of nonlinear crosstalk or idlers from the signal output port in the symmetric and asymmetric MZI-FOPAs respectively and to analyze evolution of all unwanted FWM products (idlers and nonlinear crosstalk) throughout MZI-FOPAs. Figures 2 and 3 show the simulated setups and evolution of optical spectra in each arm of both MZI-FOPA configurations.

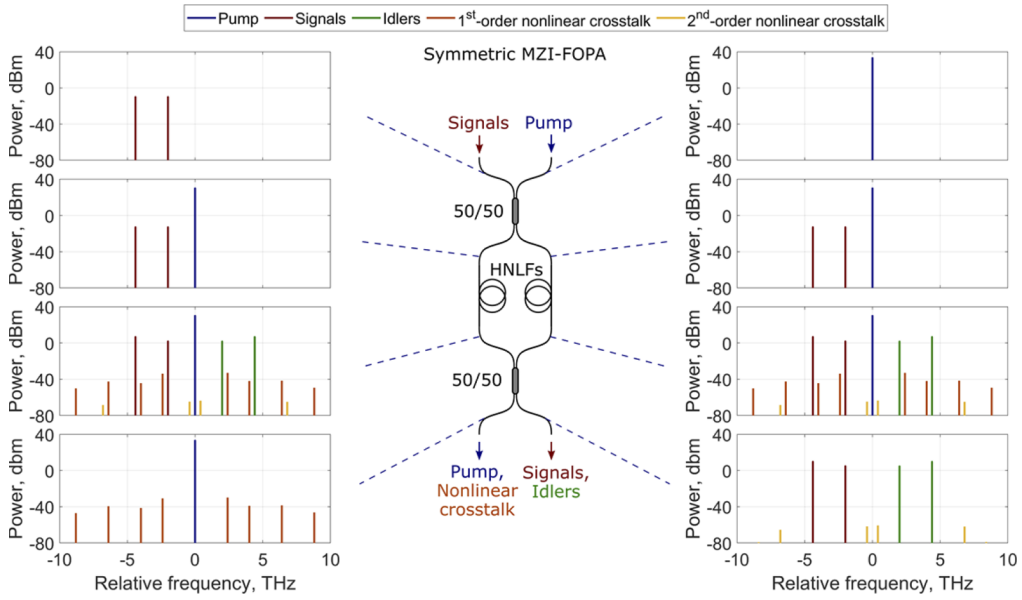

Fig. 2. Simulated optical power spectra throughout a symmetric MZI-FOPA for nonlinear crosstalk rejection. The bottom right plot shows the most significant nonlinear crosstalk products are rejected from the signal output port.

We produce two optical fields: one consisting of a single frequency pump with power of 2 W and another consisting of two single frequency signal probes with power of -10 dBm. We combine the two fields using a coupler transfer function (Eq. (5)), where ε is the power coupling coefficient, and obtain optical fields for each MZI arm. For this ideal scenario ε equals 0.5. Then, in case of the asymmetric MZI-FOPA we shift the pump phase in one of arms by $\pi/2$. We perform

Optics EXPRESS

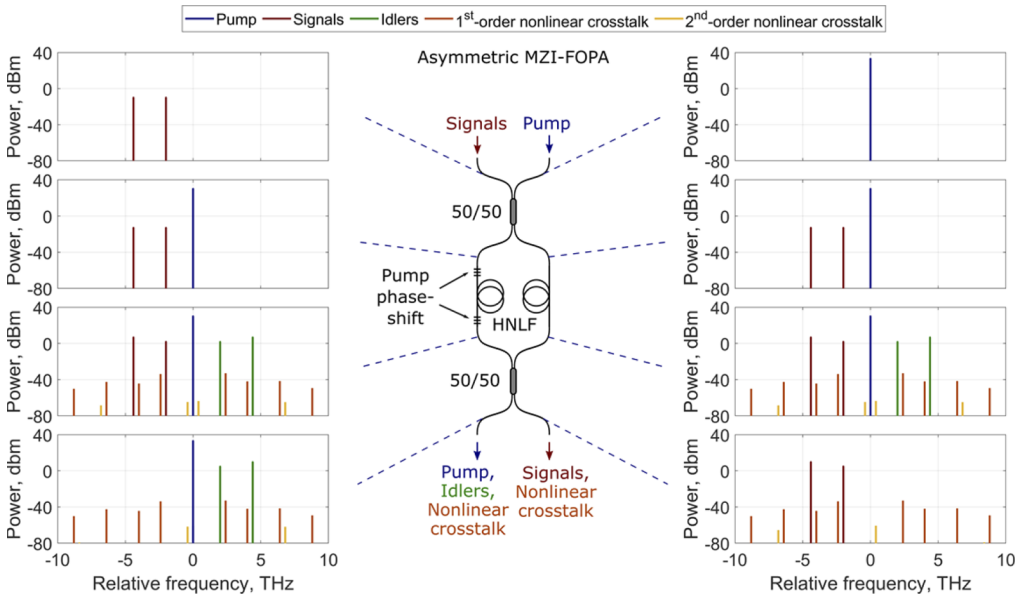

Fig. 3. Simulated optical power spectra throughout an asymmetric MZI-FOPA for idlers rejection. The bottom right plot shows the idlers are rejected from the signal output port.

split-step Fourier method transmission in a HNLF for both arms. The key simulation parameters are as follows: the pump offset from the HNLFs zero dispersion frequency is 100 GHz, the HNLFs dispersion slope is 43 s·m-3, the HNLFs nonlinearity coefficient is 14 $W^{-1}\cdot km^{-1}$, the HNLFs length is 214 m, no Raman scattering and no fiber attenuation. After fiber propagation in case of the asymmetric MZI-FOPA we shift the pump phase in the same arm by -π/2. Finally, the resulting fields are combined using the coupler transfer function again.

$$\begin{bmatrix} output_1 \\ output_2 \end{bmatrix} = \begin{bmatrix} \sqrt{1-\varepsilon} & j\sqrt{\varepsilon} \\ j\sqrt{\varepsilon} & \sqrt{1-\varepsilon} \end{bmatrix} \begin{bmatrix} input_1 \\ input_2 \end{bmatrix} \tag{5}$$

Simulation results at Fig. 2 and Fig. 3 show that in both MZI-FOPA configurations the pump and the signals are equally split and combined by the input coupler, so identical optical power spectra are injected in the HNLFs. The pump power in each arm is 1 W. Optical power spectra at the HNLF output show amplified signals, idlers, and nonlinear crosstalk products. These spectra are identical in the MZI arms in both cases regardless of the pump phase shifts in one of arms of the asymmetric MZI-FOPA. That is because phase shifts do not have an impact on optical powers, and the FWM efficiency is independent of initial phases when idlers and crosstalk products are not present at the input (this is opposed to, for example, phase-sensitive amplification, when output depends on phase matching between input waves). The difference between two MZI-FOPA configurations appear only after the output coupler, where the result of interference is defined by phase relations between waves in the MZI arms.

3.1. Symmetric MZI-FOPA for rejection of nonlinear crosstalk

The bottom-right plot at Fig. 2 shows that the most significant nonlinear crosstalk products (1st order) are cancelled at the signal output of the symmetric MZI-FOPA. They fully recombine along with the pump at the other MZI output port as expected. On the other hand, the 2nd order nonlinear crosstalk products, originating from mixing between signals and idlers, fully recombine

Optics EXPRESS

at the signal output port along with the signals and idlers. However, the power of the 2nd order crosstalk products is typically much lower than that of the 1st order products because the FWM efficiency scales with the power of involved waves and the latter involves a pump carrying the most power.

3.2. Asymmetric MZI-FOPA for rejection of idlers

The bottom-right plot at Fig. 3 shows that the idlers are cancelled at the signal output of the asymmetric MZI-FOPA. The idlers fully recombine at the pump output port of the MZI. This implies that signals could be amplified on both sides of the pump without reserving any bands for idlers, thus doubling the FOPA gain bandwidth employable for signal amplification.

The power of the 1st order nonlinear crosstalk is split equally between the two output ports, which means that only half of the total 1st order nonlinear crosstalk power is guided to the signal output port. The 2nd order nonlinear crosstalk products are split between the output ports too. The 2nd order products are derived from a combination of three signals and/or idlers, and each of them fully recombines at the signal or idler output port if they are derived from an odd number of signal or idler waves respectively. This means an equal split of the 2nd order nonlinear crosstalk products between the output ports due to a symmetry between signals and idlers. Overall, the asymmetric MZI-FOPA provides a 3 dB decrease of the total nonlinear crosstalk power at the signal output port.

4. Simulations of non-ideal MZI-FOPAs

In this section we perform a feasibility study of the proposed architecture by characterizing idler suppression in an asymmetric MZI-FOPA having non-ideal couplers and phase-shifts. The asymmetric architecture is chosen for this analysis because there are higher requirements for suppression of idlers then nonlinear crosstalk. Thus, we consider that idler suppression by at least 28 dB is required to enable idlers' frequencies to be occupied by additional signals with feasibly low performance penalties, because it corresponds to the required OSNR penalty of 0.3 dB at BER of 10^{-3} for 16QAM signals.

The same simulation model as before has been used with minor changes. The signal input was represented by a comb of single frequency probes spanning across the simulated range to observe idler suppression across the MZI-FOPA gain spectrum. Signal probe frequencies have been chosen so that no signals and the 1st order nonlinear crosstalk products occur at idler frequencies to allow for accurate measurement of suppressed idlers' powers at the signal output port. Other changes are that the pump phase shift and the power coupling coefficient ε have been varied to examine their impact on idler suppression. The phase shifts before and after HNLF were equal as the second phase shift does not affect idler suppression anyway, it is only for pump suppression at the signal output port.

The top part of Fig. 4 shows the signal gain spectrum found as a ratio between the signal probes' powers at the input and the output of the MZI. The bottom part of Fig. 4 shows the idler suppression defined as the ratio between powers of idlers and their corresponding signals at the signal output port. In the ideal case it stands at the level of around -100 dB defined by the introduced noise floor. However, in practice it is not possible to have all physical parameters exactly right, so as an example the orange curve shows idler suppression in case when the pump phase shift is 0.05 rad different from the optimal value of $\pi/2$. In this case idler suppression degrades to -26 dB. Similarly, the purple curve shows the idler suppression across the gain spectrum in the case the MZI-FOPA employs two non-ideal couplers which power coupling coefficient ε (see Eq. (5)) changes from 0.48 to 0.5 across a 10 THz range centered around the pump. This implies that coupler has both wavelength-dependent response and sub-optimal coupling coefficient of 0.49 at the pump wavelength. The idler suppression varies between

Optics EXPRESS

12 dB and 21 dB across the gain spectrum range in this case. Further we examine the impact of non-ideal phase-shift and non-ideal couplers in details.

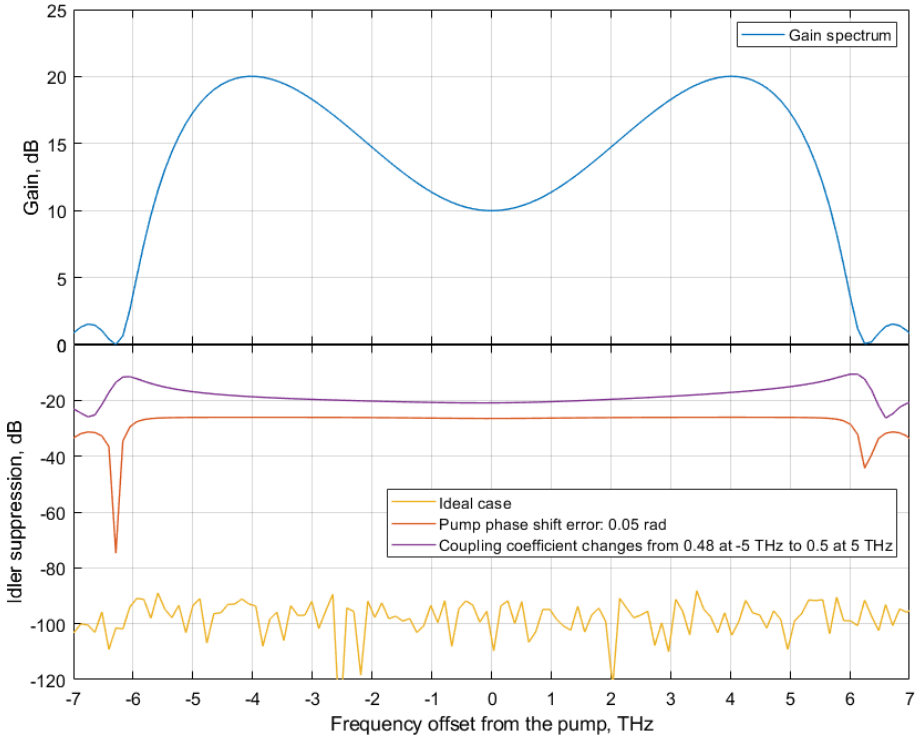

Fig. 4. Signal gain spectrum and the idler suppression ratio for three scenarios: ideal (limited by a noise floor), and non-ideal when either pump phase shift is $\pi/2 + 0.05$ rad, or couplers are non-ideal and their coupling coefficient changes linearly from 0.48 at -5 THz to 0.5 at 5 THz.

4.1. Non-ideal phase shift

Figure 5 shows the worst idler suppression ratio across the 3 dB FOPA gain bandwidth (for signals with offsets from the pump roughly between ±3 THz and ±5 THz) as a function of the pump phase shift deviations from the optimal value of $\pi/2$. Sub-optimal pump phase shifts degrade the idler suppression which means an increased idlers' power at the signal output port. The maximum tolerable phase shift error allowing for the idler suppression ratio of 28 dB is ±0.04 rad (±2.3 degrees). FBG phase shifters available in our lab have phase shift slope of ~4 rad/nm, their central wavelength can be adjusted via temperature control by 0.1 nm per 10°C, and temperature control with precision of 0.1°C is achievable, hence the pump phase shift can be set with precision of ~0.004 rad which is well within the available margin. Thus, this simulation predicts idler suppression better than 40 dB for phase shift errors <0.01 rad.

4.2. Non-ideal couplers

To analyze an impact of non-ideal couplers on the MZI-FOPA performance we assume that the input and output couplers are the same because couplers from the same batch typically have very similar performance. We consider that the coupling coefficient of real couplers has frequency dependency and might deviate from the target value of 0.5 at the FOPA central frequency. We assume however that coupling coefficient changes linearly across the range of interest. Therefore,

Optics EXPRESS

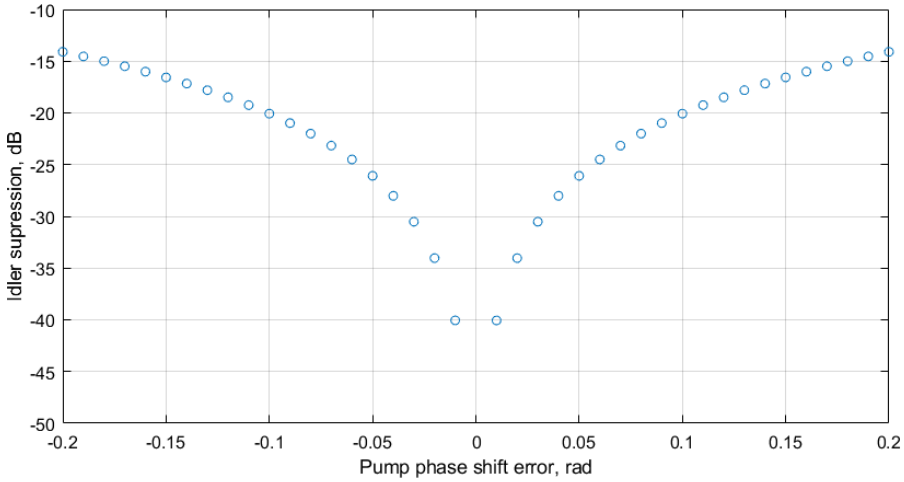

Fig. 5. The worst idler suppression across the 3 dB FOPA gain bandwidth for a range of pump phase shift deviations from the optimal value of π/2 rad.

couplers in this simulation are specified by their coupling coefficient at the pump frequency and the coupling coefficient variation across the range of interest from -5 THz to 5 THz corresponding to the 3 dB FOPA gain bandwidth (Fig. 4).

Figure 6(a) shows the worst idler suppression ratio across the 3 dB FOPA gain bandwidth for a range of non-ideal couplers in the asymmetric MZI-FOPA without alterations. The horizontal axis shows the coupling coefficient at the pump frequency, and different symbols correspond to different slopes of the coupling coefficient across the 10 THz wide range of interest. The coupling coefficient variation from 0 (flat) to 4 percent points per 10 THz is examined.

Figure 6(a) shows that the idler suppression is more sensitive to the coupling coefficient of the pump than that of the signal. Indeed, if the coupling coefficient at the pump is exactly 50%, the coupling coefficient for signal can vary in the range from 48.5% to 51.5% (variation of 3 percent points) to allow for better than 30 dB idler suppression. On the other hand, in the absence of the frequency dependency of the coupling coefficient, the pump coupling coefficient must be within 0.3 percent points from the optimal value of 50% to allow for better than 30 dB idler suppression. This is because the pump power difference in the MZI arms causes a magnified signal gain difference resulting in the amplified signal power difference and eventually a degraded idler suppression.

We have performed the same simulations for a FOPA having twice gain bandwidth as well. The pump power has been increased by a factor of 4 and the gain fiber length has been correspondingly decreased. This has scaled the FOPA gain bandwidth by a factor of two whilst having the same peak power. Importantly, this led to *exactly* the same result as shown at Fig. 6(a), i.e. the same minimum idler suppression for the same coupling coefficient at the edges of the FOPA gain bandwidth. Consequently, the maximum allowable tilt of the coupling coefficient scales inversely proportionally with the FOPA gain bandwidth.

Since deviations of the pump coupling coefficient are so detrimental to idler suppression, we consequently consider the case when a loss compensating for pump power difference is introduced to the whole field including signals in one of the MZI arms. The introduced loss coefficient was $1 - 2 * |0.5 - \varepsilon_p|$, where ε_p is the coupling coefficient at the pump frequency. Such a small attenuation (on the scale of 0.1 dB) can be introduced by bend loss, fiber strain or SMF-to-SMF splice(s). The former two options allow for tuneability, but the splice loss is more robust. Figure 6(b) shows that this technique has significantly improved idler suppression

Optics EXPRESS

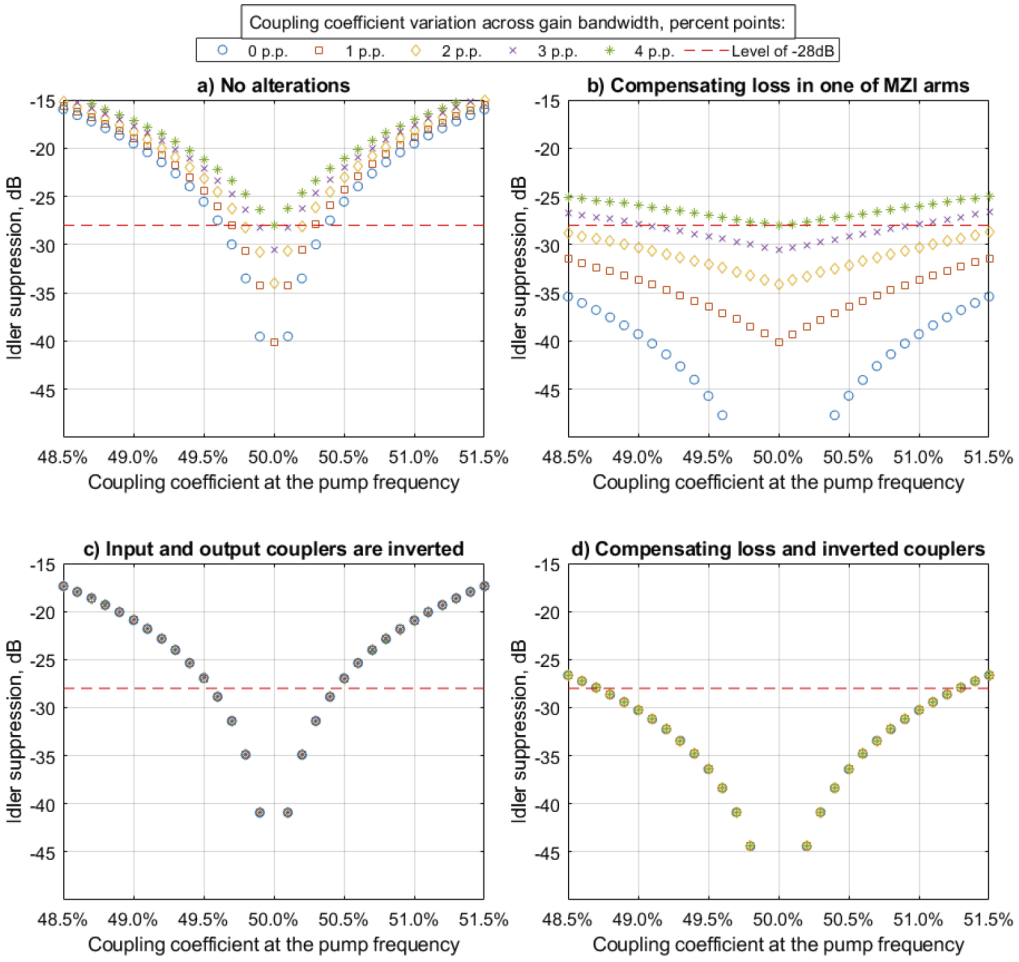

Fig. 6. The worst idler suppression across the FOPA 3 dB gain bandwidth as a function of couplers spectral characteristics for a) asymmetric MZI-FOPA without alterations, and several ways to improve performance whilst using non-ideal couplers: b) compensating loss in one of MZI arms, c) employment of input and output couplers with inverted spectral characteristics, and d) employment of both compensating loss and inverted couplers simultaneously. The red line shows the target idler suppression level of -28 dB.

Optics EXPRESS

across a wide range of pump power coupling coefficients. Thus, the compensating loss has allowed for idler suppression of at least 28 dB across the FOPA gain bandwidth for the pump coupling coefficient across the range of 3 percent points from 48.5% to 51.5% and the coupling coefficient variation across a range of up to 2 percent points. These margins are achievable with commercially available broadband couplers, although some culling might be required.

Further, we find that employment of 'inverted' couplers at the input and output of the MZI-FOPA eliminates the impact of the couplers' frequency response. 'Inverted' couplers mean that if one has a coupling coefficient $\varepsilon(f)$, the other one has the coupling coefficient $1 - \varepsilon(f)$. Note, that swapping the output ports of one of the couplers is not the same, because it swaps the phase shift as well. Figure 6(c) shows that in this case the idler suppression depends on the pump coupling coefficient only, and it is independent of the couplers' spectral characteristic. Additionally, there is a slight improvement of idler suppression as compared to the 'flat' spectral response case shown at Fig. 6(a) with blue circles. However, this technique requires a careful selection of input and output couplers' spectral properties.

Finally, we consider the case when both techniques of compensating loss and 'inverted' couplers are employed. Figure 6(d) shows improvement in this case as compared to the 'inverted' coupler alone enabling idler suppression better than 30 dB if the pump coupling coefficient is between 0.49 and 0.51. Employment of 'inverted' couplers enables virtually unlimited operation bandwidth as the impact of the coupler's spectral response is eliminated, although it can be difficult to source a pair of closely 'inverted' couplers. It is peculiar that comparison of Fig. 6(b) and (d) shows that in some cases the compensating loss alone performs better than compensating loss with 'inverted' coupler. Hence, even better performance might be possible if the asymmetric loss and the output coupler's spectral response are optimised together.

4.3. Summary on non-ideal asymmetric MZI-FOPAs

Figure 7 shows gain spectra and idler suppression for an example combination of a non-ideal phase-shift of $\pi/2 + 0.02$ rad and a non-ideal coupler which coupling coefficient varies from 0.48 to 0.5 across the range of 10 THz around the pump. This corresponds to the coupling coefficient at the pump frequency of 0.49 and variation of 2 percent points. Bottom of the Fig. 7 shows the input coupler's coupling coefficient as a function of frequency. These deviations of coupling coefficient and phase shift from optimal values are viewed as equivalent to those achievable with commercially available components. Employment of asymmetric loss reduces gain peak by ~0.6 dB due to pump attenuation but allows to improve the minimum idler suppression across the 3 dB FOPA gain bandwidth from ~20 dB in the case without alterations to ~29 dB. The employment of an inverted coupler at the output in addition to the asymmetric loss does not improve idler suppression but as it has been shown above eliminates the impact of the coupling coefficient frequency dependency thus allowing for much broader operation bandwidth for the same input coupler. In practice, even better performance can be achieved if phase shift is accurately controlled and a coupler with coupling coefficient closer to 0.5 is sourced.

Optics EXPRESS

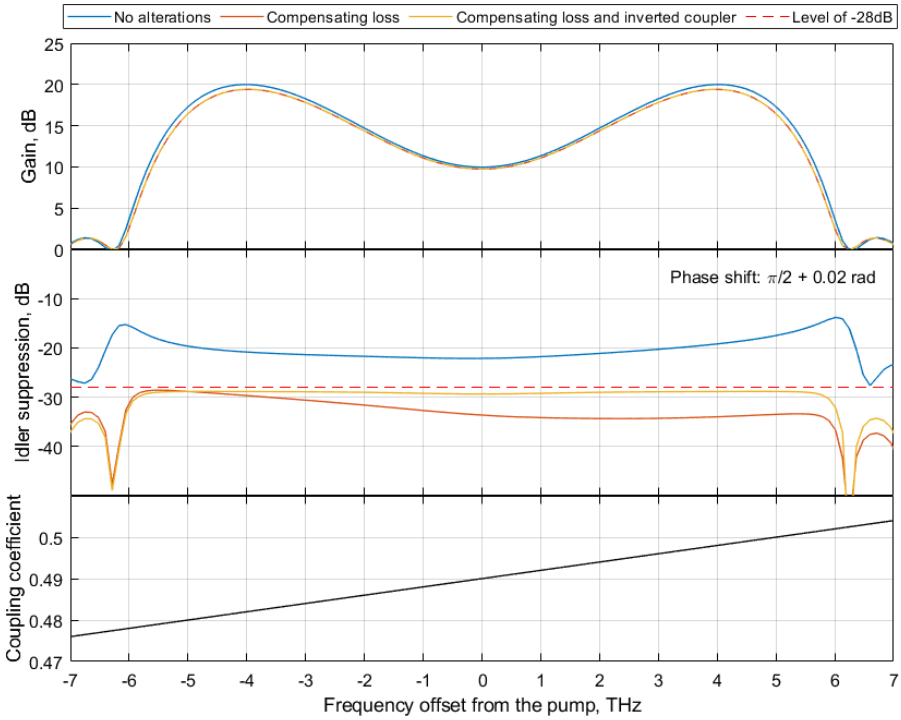

Fig. 7. Simulated gain and idler suppression spectra for an example combination of a non-ideal phase shift of $\pi/2 + 0.02$ rad and a non-ideal coupler with spectral characteristic shown at the bottom plot. Three cases are considered: MZI-FOPA without alterations, employment of compensating loss and employment of both compensating loss and an 'inverted' coupler at the MZI output. The red line shows the target idler suppression level of -28 dB.

5. Discussion

Overall, our simulations confirm that MZI-FOPAs can either suppress the 1st order nonlinear crosstalk or idlers at the signal output port. We expect based on the Shannon limit for capacity [24] that the idlers rejection allowing to double a signal bandwidth is more beneficial than the nonlinear crosstalk rejection improving a signal OSNR. However, we envisage that a practical nonlinear crosstalk reduction is easier to achieve because any crosstalk mitigation is beneficial, while rejection of idlers allowing to reuse their frequencies for signal amplification requires a high signal-to-idler extinction ratio (we estimate ~28 dB) and hence tighter margins on phase shift and coupling coefficient. Nevertheless, our simulations show that the required idlers suppression by >28 dB is experimentally possible with commercially available components. Although this arrangement is single-polarization, interferometric FOPAs can be placed in arms of a Mach-Zehnder-like polarization diversity arrangement for polarization-insensitive operation [23].

Interferometric rejection of idlers has implications well beyond doubling the available FOPA gain bandwidth. Interferometric wavelength converters and optical phase conjugators can produce signal copies within the signal band and have a dedicated output port for them where original signals are suppressed. Interferometric wavelength converters can therefore avoid blocked wavelengths when converting WDM channels especially in a tuneable manner. Similarly,

Optics EXPRESS

interferometric optical phase conjugators can be used for a waveband-shift-free optical phase conjugation [25].

6. Conclusions

We have presented and simulated two interferometric FOPA configurations for rejection of unwanted four wave mixing products. The symmetric interferometric FOPA provides suppression of the most significant nonlinear crosstalk products, and we believe this design is readily adaptable for phase-sensitive amplifiers, wavelength converters and optical phase conjugators. The asymmetric interferometric FOPA suggests a paradigm shifting ability to reject idlers from the signal output port and thus to enable idlers' frequencies for signal amplification. The interferometric idlers' rejection can therefore double the bandwidth employable for signal amplification in FOPA. The asymmetric architecture has implications beyond FOPAs too. For example, it allows for a waveband-shift free optical phase conjugation and a flexible all-optical wavelength conversion unrestricted by an overlap between signals' and their copies' frequencies. Moreover, both interferometric architectures improve noise figure, reduce insertion loss and allow for a great pump wavelength tuneability by removing the need for lossy wavelength selective combiners and filters for the pump and the signals.

In addition, we have examined two simple techniques enabling high suppression ratio for unwanted four wave mixing products across wide bandwidth whilst employing real-world couplers in the interferometer. Therefore, the simulations presented here illustrate the power and practicality of the proposed designs by demonstrating that practical pump phase shifters and couplers allow to suppress idlers by >28 dB across bandwidth of at least 10 THz which is sufficient for 16QAM signals to reuse idler frequencies with penalty <0.3 dB at BER of 10^{-3}.

Funding. Engineering and Physical Sciences Research Council (EP/R024057/1 (FPA-ROCS), EP/S003436/1 (PHOS), EP/S016171/1 (EEMC)); UK Research and Innovation (Future Leaders Fellowship MR/T041218/1).

Disclosures. The authors declare no conflicts of interest.

Data availability. Data underlying the results presented in this paper are available in Ref. [26].

References

1. A. Ferrari, A. Napoli, J. K. Fischer, N. Costa, A. D'Amico, J. Pedro, W. Forysiak, E. Pincemin, A. Lord, A. Stavdas, J. P. F.-P. Gimenez, G. Roelkens, N. Calabretta, S. Abrate, B. Sommerkorn-Krombholz, and V. Curri, "Assessment on the Achievable Throughput of Multi-Band ITU-T G.652.D Fiber Transmission Systems," IEEE J. Light. Technol. **38**(16), 4279–4291 (2020).
2. J. Hansryd, P. A. Andrekson, M. Westlund, J. Li, and P. O. Hedekvist, "Fiber-based optical parametric amplifiers and their applications," IEEE J. Sel. Top. Quantum Electron. **8**(3), 506–520 (2002).
3. M. E. Marhic, K. K. Y. Wong, and L. G. Kazovsky, "Wide-band tuning of the gain spectra of one-pump fiber optical parametric amplifiers," IEEE J. Sel. Top. Quantum Electron. **10**(5), 1133–1141 (2004).
4. V. Gordienko, M. F. C. Stephens, A. E. El-Taher, and N. J. Doran, "Ultra-flat wideband single-pump Raman-enhanced parametric amplification," Opt. Express **25**(5), 4810–4818 (2017).
5. M. Jamshidifar, A. Vedadi, and M. E. Marhic, "Continuous-wave one-pump fiber optical parametric amplifier with 270 nm gain bandwidth," in *35th European Conference on Optical Communication* (ECOC 2009), paper 1.1.4.
6. J. M. C. Boggio, S. Moro, E. Myslivets, J. R. Windmiller, N. Alic, and S. Radic, "155-nm Continuous-Wave Two-Pump Parametric Amplification," IEEE Photonics Technol. Lett. **21**(10), 612–614 (2009).
7. H. Sakr, T. D. Bradley, G. T. Jasion, E. N. Fokoua, S. R. Sandoghchi, I. A. Davidson, A. Taranta, G. Guerra, W. Shere, Y. Chen, J. R. Hayes, D. J. Richardson, and F. Poletti, "Hollow Core NANFs with Five Nested Tubes and Record Low Loss at 850, 1060, 1300 and 1625 nm," in *Optical Fiber Communications Conference* (OFC 2021), paper F3A.4.
8. C. B. Gaur, V. Gordienko, A. A. I. Ali, P. Hazarika, A. Ellis, and N. J. Doran, "Polarization- insensitive fibre optic parametric amplifier with gain bandwidth of 35 nm in L-band," in *European Conference on Optical Communication* (ECOC 2021).
9. V. Gordienko, C. B. Gaur, F. Bessin, I. D. Phillips, and N. J. Doran, "Robust polarization-insensitive C & L band FOPA with >17 dB gain for both WDM and bursty traffic," in *Optical Fiber Communications Conference and Exhibition* (OFC 2021), paper M5B.3.
10. M. Jamshidifar, A. Vedadi, and M. E. Marhic, "Reduction of Four-Wave-Mixing Crosstalk in a Short Fiber-Optical Parametric Amplifier," IEEE Photonics Technol. Lett. **21**(17), 1244–1246 (2009).

Optics EXPRESS

11. K. R. H. Bottrill, N. Taengnoi, H. Liu, R. Kakarla, Y. Hong, and P. Petropoulos, "Suppression of Spurious Mixing in FWM-based Systems through Mid-Span Pump Phase Shift," in *Optical Fiber Communications Conference and Exhibition* (OFC 2022), paper W4J.2.
12. V. Gordienko, F. M. Ferreira, V. Ribeiro, and N. Doran, "Suppression of Nonlinear Crosstalk in a Polarization Insensitive FOPA by Mid-Stage Idler Removal," in *Optical Fiber Communications Conference and Exhibition* (OFC 2019), paper M4C.4.
13. V. Gordienko, F. M. Ferreira, C. B. Gaur, and C. J. Doran, "Looped Polarization-Insensitive Fiber Optical Parametric Amplifiers for Broadband High Gain Applications," IEEE J. Light. Technol. **39**(19), 6045–6053 (2021).
14. K. Mori, T. Morioka, and M. Saruwatari, "Optical parametric loop mirror," Opt. Lett. **20**(12), 1424–1426 (1995).
15. W. Imajuku and A. Takada, "Noise figure of phase-sensitive parametric amplifier using a Mach-Zehnder interferometer with lossy Kerr media and noisy pump," IEEE J. Quantum Electron. **39**(6), 799–812 (2003).
16. V. Ribeiro and A. M. Perego, "Parametric amplification in lossy nonlinear waveguides with spatially dependent coupling," Opt. Express **30**(10), 17614–17624 (2022).
17. S. Trillo, S. Wabnitz, G. I. Stegeman, and E. M. Wright, "Parametric amplification and modulational instabilities in dispersive nonlinear directional couplers with relaxing nonlinearity," J. Opt. Soc. Am. B **6**(5), 889–900 (1989).
18. A. Mecozzi, "Parametric amplification and squeezed-light generation in a nonlinear directional coupler," Opt. Lett. **13**(10), 925–927 (1988).
19. V. Ribeiro, M. Karlsson, and P. Andrekson, "Parametric amplification with a dual-core fiber," Opt. Express **25**(6), 6234–6243 (2017).
20. M. E. Marhic, *Fibre optical parametric amplifiers, oscillators and related devices* (Cambridge University, 2008).
21. S. Takasaka, Y. Taniguchi, M. Takahashi, J. Hiroshi, M. Tadakuma, H. Matsuura, K. Doi, and R. Sugizaki, "Quasi phase-matched FOPA with 50 nm gain bandwidth using dispersion stable highly nonlinear fiber," in *Optical Fiber Communications Conference* (OFC 2014), paper W3E.2.
22. M. Jazayerifar, I. Sackey, R. Elschner, T. Richter, L. Molle, P. W. Berenguer, C. Schubert, K. Jamshidi, and K. Petermann, "Impact of Brillouin Backscattering on Signal Distortions in Single-Fiber Diversity Loop Based Polarization-Insensitive FOPAs," J. Lightwave Technol. **35**(19), 4137–4144 (2017).
23. F. Bessin, V. Gordienko, F. M. Ferreira, and N. Doran, "First Experimental Mach-Zehnder FOPA for Polarization- and Wavelength-Division-Multiplexed Signals," in *European Conference on Optical Communication* (ECOC 2021).
24. C. E. Shannon, "Communication in the Presence of Noise," Proc. IRE **37**(1), 10–21 (1949).
25. I. Sackey, C. Schmidt-Langhorst, R. Elschner, T. Kato, T. Tanimura, S. Watanabe, T. Hoshida, and C. Schubert, "Waveband-Shift-Free Optical Phase Conjugator for Spectrally Efficient Fiber Nonlinearity Mitigation," J. Lightwave Technol. **36**(6), 1309–1317 (2018).
26. V. Gordienko, F. M. Ferreira, V. Ribeiro, and N. J. Doran, "Design of interferometric fiber optic parametric amplifier for unwanted four-wave mixing products (idlers, crosstalk) rejection," Aston University (2023). https://doi.org/10.17036/researchdata.aston.ac.uk.00000548.